Focal Mechanism of Earthquakes and Three-Dimentional Finite Element Model of Seismogenic Stress Field in Taiwan Region

AUTHOR(S):

Xu, Jiren

CITATION:

Xu, Jiren. Focal Mechanism of Earthquakes and Three-Dimentional Finite Element Model of Seismogenic Stress Field in Taiwan Region. Memoirs of the Faculty of Science, Kyoto University. Series of physics, astrophysics, geophysics and chemistry 1994, 39(1): 23-47

ISSUE DATE:

1994-03

URL:

http://hdl.handle.net/2433/257626

Memoirs of the Faculty of Science, Kyoto University, Series of Physics, Astrophysics, Geophysics and Chemistry, Vol. XXXIX, No. 1, Article 2, 1994

Focal Mechanism of Earthquakes and Three-Dimentional Finite Element Model of Seismogenic Stress Field in Taiwan Region

By

Jiren XU

Department of Geophysics, Faculty of Science, Kyoto University, Kyoto 606-01, Japan

(Received November 5, 1993)

Abstract

Characteristics of stress field in and around the Taiwan region have been analyzed based on focal mechanism solutions. Different types of stress field are revealed in the eastern coastal region along the Longitudinal Valley fault, and in Hualian and the northeastern sea region. Based on the seismogenic stress field simulated from the three-dimensional finite element model established in this study, the conclusions are:

(1) There is a compressive stress field in the WNW-ESE direction along the Longitudinal Valley fault, in the central and western region west of the Longitudinal Valley fault. It is attributed to the compressive force in the WNW-ESE direction generated by the collision movement between the Philippine Sea and the Eurasian plates. Shallow earthquakes with reverse faulting type dominate the seismic activity along the fault. (2) There is the northward-dipping subduction zone of the Philippine Sea plate moving to the Eurasian plate in the northeastern sea region off Hualian. A down-dip extensional stress field exists within the slab from the surface to depth of about 200 km, which results from the gravitational force due to density difference between the slab and its surrounding, and the thermal stresses on the slab caused by the contact with a hot asthenosphere. At the depth of about 300 km, the stress in the slab changes from the down-dip extension too the down-dip compression. It may come from the lower compression of the strong material. The stress fild model explains why a tensile stress field in the N-S direction dominates in the shallow part and the normal faulting earthquakes occur there. (3) The Hualian region is located at a cross of boundaries, i.e. the collision zone along the Longitudinal Valley fault and the subduction zone under the northeastern sea region off Hualian, and is a high seismically zone as well as a complex stress pattern zone.

1. Introduction

Taiwan is located along a convergent boundary between the Eaurasian and Philippine Sea plates. The Philippine Sea plate is moving toward the Eurasian plate. The relative convergence rate at Taiwan is about 6.8 cm/yr with an azimuth 310° (Seno, 1977 and Pezzopane et al., 1989) (Fig. 1). The convergence movement between the two plates causes the Taiwan region to be one of the most tectonically and seismically active regions in the world. Most large events concentrate in two regions of Taiwan, the Longitudinal Valley fault region and the Hualian region located from the northern part of Longitudinal Valley fault to the northeastern sea region off Hualian.

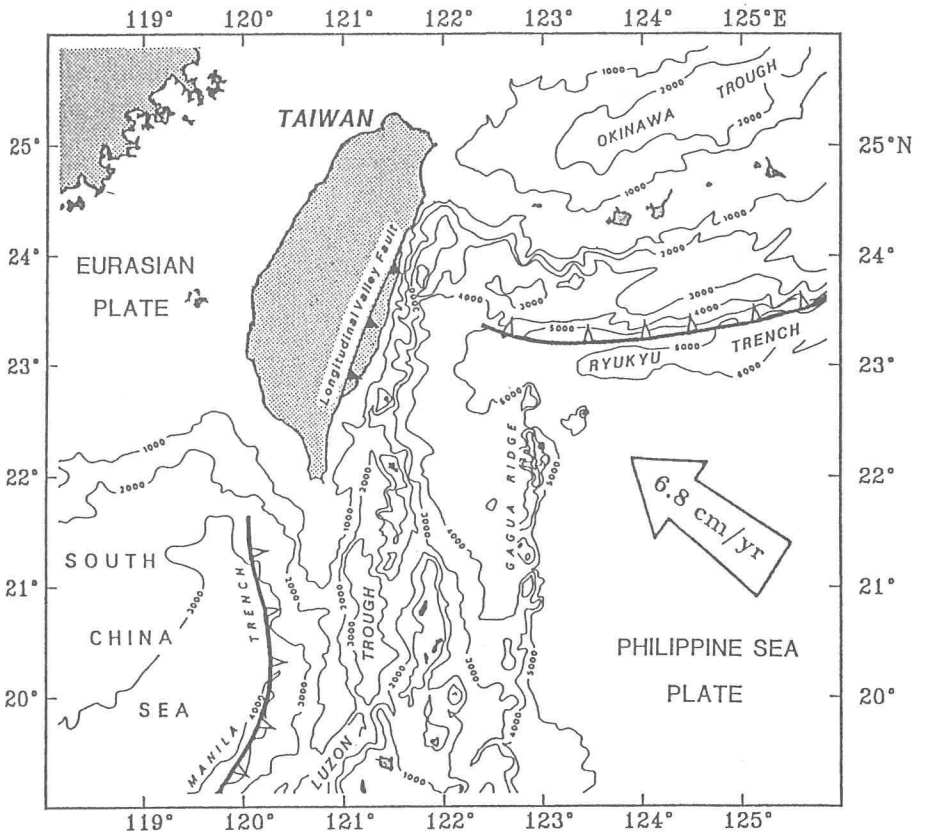

Fig. 1. Regional map showing major tectonic features in and around Taiwan. Longitudinal Valley fault is a main convergent boundary between the Philippine Sea plate and the Eurasian plate there. Large arrow means relative moving direction and rate of the Philippine Sea plate toward the Eurasian plate (from Pezzopane et al., 1989).

The Longitudinal Valley fault located along the eastern coast is the largest fault in Taiwan, which is a convergent boundary between the Eurasian and the Philippine Sea plates (Hsu, 1990). It stretches from Taidong in the southernend of the eastern coast, through Fuli and Yuli regions of the central part of Taiwan to Hualian in the northernend of the eastern coast. The fault region runs more than 150 km in length and from 2 to 7 km in width. The thrust fault with a minor strike-slip component trends toward N20°E and dips to 70°E (Yu et al, 1990, and Ho, 1986). The eastern wall of the fault is the hanging wall. The Philippine Sea plate thus moves northwestward and thrusts upon the Eurasian plate along the fault. In the Hualian region and the northeastern sea region off Hualian, the Philippine Sea plate seems to change the direction to the north (Wang, 1984). Many large earthquakes occurred in and around Hualian region recently.

The crustal movement along the Longitudinal Valley fault has been investigated by some authors. Crustal movements in the three regions, i.e. Taidong, Yuli and Hualian, have been surveyed frequently using triangulation and leveling networks from

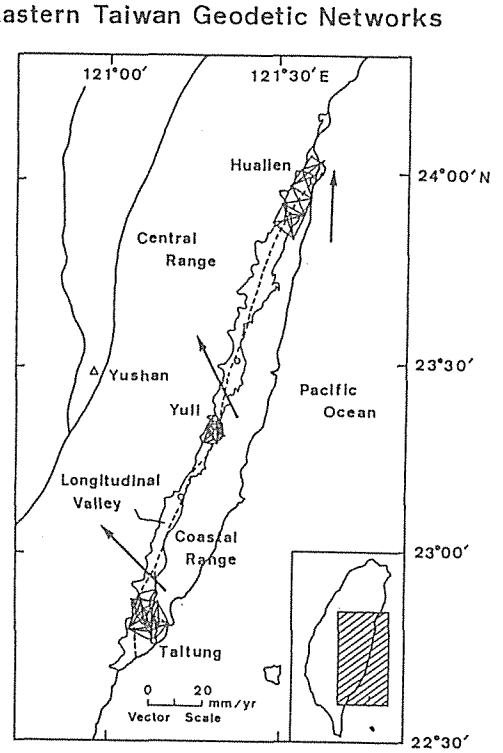

Fig. 2. Horizontal crustal movements along the Longitudinal Valley fault at Taidong, Yuli and Hualian regions (from Yu et al., 1990).

1983 to 1988 (Yu, et al., 1990). The results show that the rate of relative horizontal motion between the Coastal Range block and the Central Range block changes from 34 mm/yr in the N46°W direction at the Taidong region to 25 mm/yr in the N-S direction at the Hualian region. The rate at the Yuli region has an intermediate value of 33 mm/yr in N27°W (Fig. 2). Moreover, a significant vertical motion is observed in the Yuli region. In the Coastal Range the rate of uplifting is about 20 mm/yr, the largest observed value along the Longitudinal Valley fault.

In the Ilan region to the north of the Hualian region (in the northeastern region of Taiwan), the crustal movement has been measured by triangulation and leveling surveys. The main observation is the crustal subside by 20 cm during the period between 1920 and 1976 which is characterized by tensile strain field in the NW-SE direction (Sheu, 1987). The vertical crustal movement is quite different from that along the Longitudinal Valley fault.

Earthquake focal mechanisms and the seismogenic stress field in Taiwan were presented by Tsai (1986) and Angelier et al. (1986). Seismicity in Taiwan is probably caused by the relative convergence between the Eurasian and Philippine Sea plates, which produces crustal deformation in Taiwan.

The studies as mentioned above are, however, rather qualitative. Thus, it is necessary to investigate more quantitative correlations between the seismogenic stress field and the crustal movement associated with the Philippine Sea plate. The focal

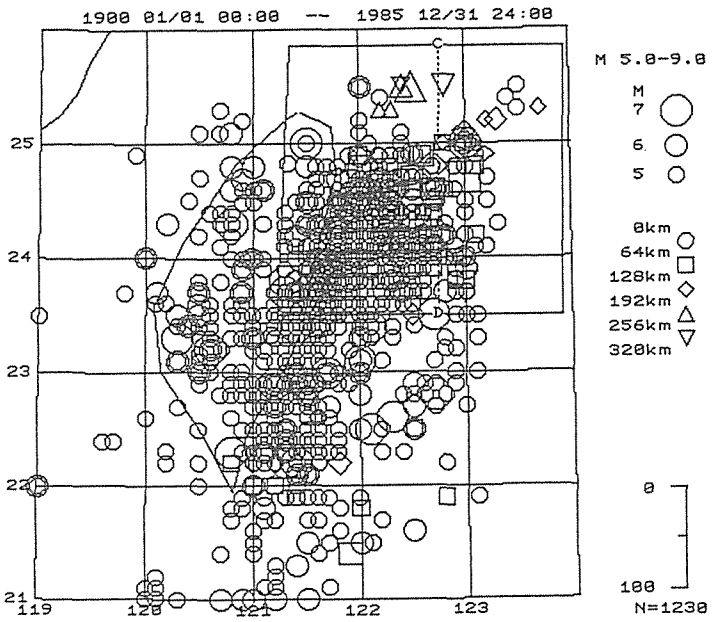

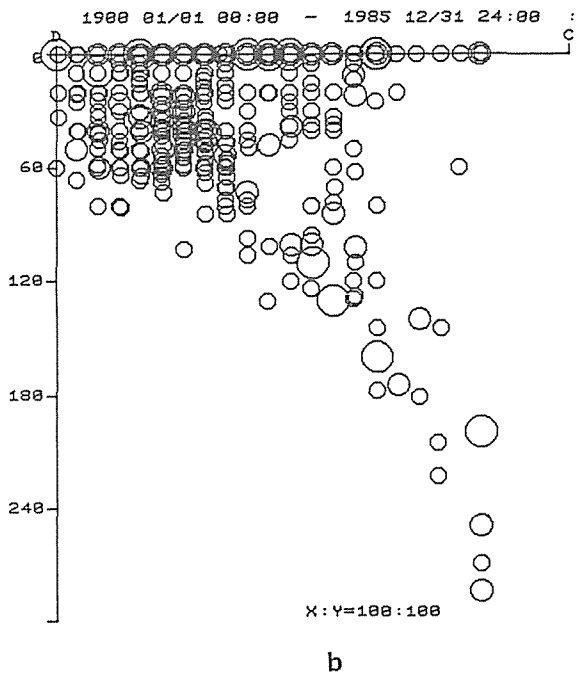

Fig. 3. (a) Epicentral distribution of earthquakes occurred during from 1900 to 1985 (M≧5) in Taiwan region. (b) Hypocentral distribution on the vertical section along CD line shown in Fig. 3(a) in the subduction zone in the northeastern sea region off Hualian.

mechanism solutions of shallow and intermediate-deep earthquakes have already been determined and reported in the Taiwan region. In order to reveal the quantitative relation between the focal mechanism and plate movement, a two-dimensional numerical approach seems insufficient. A three dimensional finite element modeling is, thus, employed to obtain more precise information with respect to the stationary stress regime in Taiwan region. In this study, the seismicity and mechanism solutions of earthquakes in Taiwan are analyzed at first. The seismogenic stress field in the Longitudinal Valley fault and the northeastern sea region off Hualian are investigated. Based on mechanism solutions of earthquakes, a model of seismogenic stress field in Taiwan will be established by a three dimensional finite element method.

2. Characteristics of Seismicity and Mechanism Solutions of Earthquakes

The epicentral distribution of earthquakes ($M \geqq 5$) in and around Taiwan from 1900 to 1985 is shown in Fig. 3. Data employed for the present study are as follows: (1) Seismological Catalogue of China (1831 B.C.–1969 A.D.) (Gu et al., 1983(a)); (2) Seismological Catalogue of China (1970–1979) (Gu et al., 1983(b)); (3) Seismological Almanac of China in 1982 (data from 1980 to 1982) (Group for Seismological Almanac of China, 1985). Characteristics of temporal variations of seismicity derived from the above data represented strong seismo-tectonic relations between Taiwan region and other regions in East Asia (Zhao et al., 1990). Many shallow reverse faulting events whose depths are less than 70 km occur along the Longitudinal Valley fault. Intermediate-depth earthquakes, however, occur beneath the Hualian and the northeastern sea region off Hualian besides shallow earthquakes. A vertical profile of the hypocenters along the N-S direction in and around Hualian is shown in Fig. 3(b). The deepest event occurred at the depth of 285 km (Fig. 3(b)). Seismicity in this region clearly shows an north-dipping Wadati-Benioff zone in the north of 24°N. This wadati-Benioff zone has a thickness of about 60 km and begins to deepen along 24°N at dip angle of 45° to 50°. The leading edge reaches a depth of about 300 km at about 25.5°N. The presence of this seismic zone implies that subduction of the Philippine Sea plate under the Eurasian plate extends from south to north in the northeastern sea region of Taiwan.

In order to clarify characteristics of mechanisms of earthquakes in the Taiwan region and its surroundings, the mechanism solutions of 103 large and moderate-size earthquakes listed in Table 1 have been analyzed in this study. The Harvard centroid moment tensor solutions (CMT) (for example Dziemonski et al., 1983(a) and 1983(b)) for earthquakes from 1977 to 1989 are used in this study. Some mechanism solutions are used in this study reported by Yan et al., (1979), Zhuo et al., (1983), Wang et al., (1985) and Ishikawa (1993). Methods to analyze properties of focal mechanisms in the subregions and their relationship with stress field are same as those used by Xu et al. (1988).

Based on the orientations of principal compressional axes (P-axes), principal tensile axes (T-axes) and null axes (N-axes) of shallow earthquakes in Taiwan, three seismic active regions are defined as shown in Fig. 4, being the southeastern region

Table 1. List of earthquake mechanism solutions used in this study

Date	Origin Time	Lat. (°N)	Long. (°E)	Depth (km)	M	N-axes Az. Pl.	P-axes Az. Pl.	T-axes Az. Pl.	Ref.*
1963 2 13	8:50	24 36	122 6	47	7.0	73 15	168 19	307 65	1
1964 1 18	12: 4	23 5	120 35	18	6.0	337 81	99 5	190 8	2
1964 11 26	18:21	24 55	122 2	17	6.0	297 0	27 53	207 37	4
1965 4 27	6:15	21 0	120 41	29	6.0	188 0	278 59	98 31	3
1966 3 12	16:31	24 14	122 40	42	6.5	114 54	243 25	345 25	3
1966 3 13	0:31	24 30	123 0	42	7.8	308 0	218 35	38 55	2
1966 3 23	8: 4	23 52	122 58	40	6.0	160 74	66 1	336 16	3
1968 2 26	18:50	22 46	121 28	8	6.5	34 19	302 6	185 69	3
1972 1 4	3:16	22 30	122 4	6	6.7	178 32	85 5	346 57	3
1972 1 25	10: 6	22 34	122 22	29	6.3	0 90	116 0	26 0	3
1972 4 17	18:49	24 6	122 26	48	6.1	60 8	154 27	314 62	4
1972 4 24	17:57	23 36	121 33	29	6.0	156 22	247 2	340 68	4
1972 11 8	22:25	23 54	121 36	36	5.9	217 0	127 5	307 85	2
1972 11 10	2:41	23 48	121 36	22	6.3	231 29	133 14	21 57	2
1975 3 23	7:32	22 44	122 48	21	6.6	328 83	103 5	193 5	3
1975 5 24	0:01	22 42	122 34	6	6.2	320 84	95 4	185 4	3
1977 1 7	19:36	21 10	120 17	33	5.7	349 13	225 67	84 18	9
1977 7 15	2:12	24 3	122 13	33	5.5	68 8	164 38	329 51	9
1977 10 19	22:39	22 37	121 37	158	5.5	8 17	157 70	275 10	9
1978 2 8	0:15	24 9	122 40	40	5.5	244 0	154 42	334 48	9
1978 3 14	20:32	24 4	122 38	43	5.5	64 9	161 36	322 53	9
1978 4 29	19:25	24 40	122 43	18	5.4	136 74	292 15	24 6	9
1978 7 23	14:42	22 17	121 31	17	6.5	16 18	110 13	234 67	3
1978 8 9	18:35	23 31	121 28	22	5.2	290 21	183 38	42 45	1
1978 9 2	1:57	24 54	121 59	109	6.1	158 24	260 27	32 53	9
1978 9 10	16:34	24 7	121 43	15	5.4	270 20	170 28	32 55	9
1978 12 23	11:23	23 36	122 6	33	7.0	268 45	358 2	91 54	1
1979 12 2	5:25	22 55	121 27	37	5.5	21 21	290 4	188 69	9
1980 3 21	8:59	22 57	121 26	24	5.2	20 19	288 4	187 70	9
1980 10 18	0: 8	24 17	121 55	24	5.0	26 12	126 41	283 47	9
1980 11 7	12:36	24 4	122 19	33	5.4	70 12	167 33	322 55	9
1981 1 29	4:51	24 31	121 56	33	5.6	185 38	61 35	304 33	9
1981 2 10	15:11	23 53	123 23	41	5.2	39 5	131 25	299 65	9
1981 2 20	20: 9	22 55	121 27	26	5.4	224 5	132 18	327 71	9
1981 3 2	12:13	22 53	121 27	24	5.5	19 18	287 7	177 71	9
1981 6 28	8: 1	21 16	121 50	122	5.3	268 2	178 5	16 85	9
1982 1 23	14:10	23 50	121 39	33	5.6	39 10	137 39	298 49	9
1982 10 20	20: 1	23 50	121 54	28	5.4	228 13	133 20	349 66	9
1982 12 17	2:43	24 38	122 37	73	6.2	183 42	284 12	27 45	9
1983 4 26	15:26	24 38	122 33	123	5.6	282 14	178 43	26 44	9
1983 5 10	0:15	24 25	121 35	33	5.7	158 7	298 81	67 5	9
1983 6 21	14:48	24 15	122 29	24	5.8	102 15	197 19	337 65	9
1983 6 24	9: 6	24 12	122 26	54	6.0	92 10	186 23	340 65	9
1983 6 25	14:12	23 5	123 20	24	5.4	135 47	270 34	17 23	9
1983 6 25	19:40	24 0	122 33	42	5.5	264 4	171 35	0 55	9
1983 9 7	23:11	24 5	122 23	33	5.5	69 10	166 36	325 53	9
1983 9 9	17: 1	24 5	122 22	33	5.3	97 9	191 22	346 66	9
1983 9 21	19:20	24 7	122 13	33	6.0	75 10	172 34	331 54	9
1983 9 23	12:29	24 0	122 13	33	5.7	71 17	173 36	321 49	9
1983 10 7	20: 5	23 58	122 35	33	5.1	19 5	110 10	262 79	9
1984 1 19	11:12	24 7	122 19	41	5.1	71 54	199 24	301 25	9
1984 2 13	4:48	25 26	122 23	286	5.5	290 6	30 60	196 29	9
1984 3 28	9:11	24 5	122 39	39	5.5	72 12	169 29	322 58	9
1984 4 19	17:29	24 53	122 25	33	5.2	254 13	110 74	347 9	9

Table 1. List of earthquake mechanism solutions (continue)

Date	Origin Time	Lat. (°N)	Long. (°E)	Depth (km)	M	N-axes Az.	N-axes Pl.	P-axes Az.	P-axes Pl.	T-axes Az.	T-axes Pl.	Ref.*
1984 8 29	14:12	24 46	122 47	142	5.1	61	1	152	53	330	36	9
1984 12 29	1: 6	24 56	122 8	33	5.4	164	39	279	28	35	39	9
1985 1 13	21:51	24 7	122 28	39	5.8	170	30	269	15	22	56	9
1985 2 18	18:41	23 19	122 43	37	5.5	161	79	284	6	15	9	9
1985 2 18	19:41	23 21	123 17	44	5.7	161	79	284	6	15	9	9
1985 6 12	17:22	24 29	122 5	33	5.2	101	48	290	42	196	5	9
1985 9 20	15: 1	24 36	122 19	33	5.3	267	5	162	71	358	18	9
1986 1 16	13: 4	24 44	122 6	33	5.5	58	3	158	72	328	17	9
1986 2 27	6:23	24 4	122 18	33	5.8	71	9	167	31	326	57	9
1986 3 22	4:45	23 25	121 35	33	5.6	20	22	113	61	216	67	9
1986 3 22	10:31	24 44	122 55	33	5.2	114	34	272	54	16	10	9
1986 3 22	11:19	24 42	122 47	33	5.3	172	69	272	4	3	20	9
1986 3 22	12: 6	24 43	122 55	33	5.3	93	30	306	56	192	15	9
1986 3 22	14:27	24 35	122 57	33	4.9	86	1	179	65	355	25	9
1986 3 22	18:45	24 46	123 14	33	5.3	276	31	94	59	185	1	9
1986 3 25	12:13	24 48	123 14	33	5.1	273	2	10	75	183	15	9
1986 5 20	5:25	24 2	121 36	33	6.2	230	16	140	2	43	74	9
1986 6 2	14:21	24 2	123 23	32	5.2	66	5	157	8	307	81	9
1986 6 4	16:21	23 58	121 46	25	5.2	34	16	129	17	264	66	9
1986 7 30	11:31	24 37	121 48	33	5.6	43	13	196	75	312	7	9
1986 7 31	11:36	24 52	122 43	33	5.1	299	4	164	84	30	4	9
1986 8 11	8: 5	22 15	121 40	129	5.4	340	21	247	7	140	68	9
1986 11 14	21:20	23 58	121 49	33	6.2	212	1	122	12	308	77	9
1986 11 15	7:24	23 49	121 40	33	5.5	5	37	125	34	244	35	9
1986 12 10	23:55	24 59	121 51	103	5.3	2	22	259	30	122	51	9
1987 1 6	5: 7	23 59	121 47	38	5.8	13	12	278	20	132	67	9
1987 4 11	18:13	23 59	122 5	33	5.6	13	21	201	68	104	3	9
1987 6 12	9:51	25 27	122 8	265	5.4	166	9	326	81	76	3	9
1987 6 21	1:49	22 12	123 52	33	4.9	28	18	295	9	178	70	9
1987 6 27	7:38	24 17	121 44	35	5.2	359	14	227	70	93	14	9
1987 10 14	7:37	21 16	121 52	100	5.2	260	18	157	35	12	49	9
1987 11 18	12: 4	24 58	123 56	120	4.9	241	54	30	32	130	14	9
1987 12 18	5:53	23 12	121 2	33	5.0	209	79	305	1	35	11	9
1988 2 12	19:15	23 52	122 28	32	5.6	14	45	187	45	281	4	9
1988 4 7	3: 5	23 55	121 40	33	5.2	216	7	124	19	325	70	9
1988 4 24	20: 3	23 26	121 49	44	5.6	214	17	307	8	62	71	9
1988 7 20	23:15	23 53	121 35	44	5.8	30	16	125	15	255	67	9
1988 8 9	16:51	24 13	122 20	48	5.3	165	20	261	17	29	63	9
1988 8 11	3:40	21 55	121 25	41	5.4	290	47	187	12	86	41	9
1988 8 19	18:10	24 42	122 30	99	5.2	171	17	268	23	46	61	9
1988 8 28	15:34	24 4	122 25	45	5.2	81	2	172	16	343	74	9
1988 9 18	15:38	24 32	122 19	83	5.3	188	10	278	1	13	80	9
1988 10 16	12: 9	21 50	121 45	33	5.3	250	62	118	20	20	19	9
1988 12 27	18:51	24 1	122 49	25	5.1	347	45	171	45	79	2	9
1989 4 4	20:10	25 1	123 21	141	5.1	73	19	332	28	192	55	9
1989 5 15	18: 5	24 5	122 17	50	5.2	129	33	221	3	316	57	9
1989 8 3	11:31	23 1	122 1	10	5.9	71	66	282	21	187	11	9
1989 8 21	23:12	24 5	122 30	41	5.6	82	9	177	29	336	59	9
1989 9 23	17:51	22 37	122 2	31	5.5	170	51	283	18	25	33	9

*1: Wang et al. (1985)
2: Yan et al (1979)
3: Zhuo et al. (1983)
4: Ishikawa (1993)
9: Harvard CMT solutions (Dziemonski et al., 1983(a) and so on)

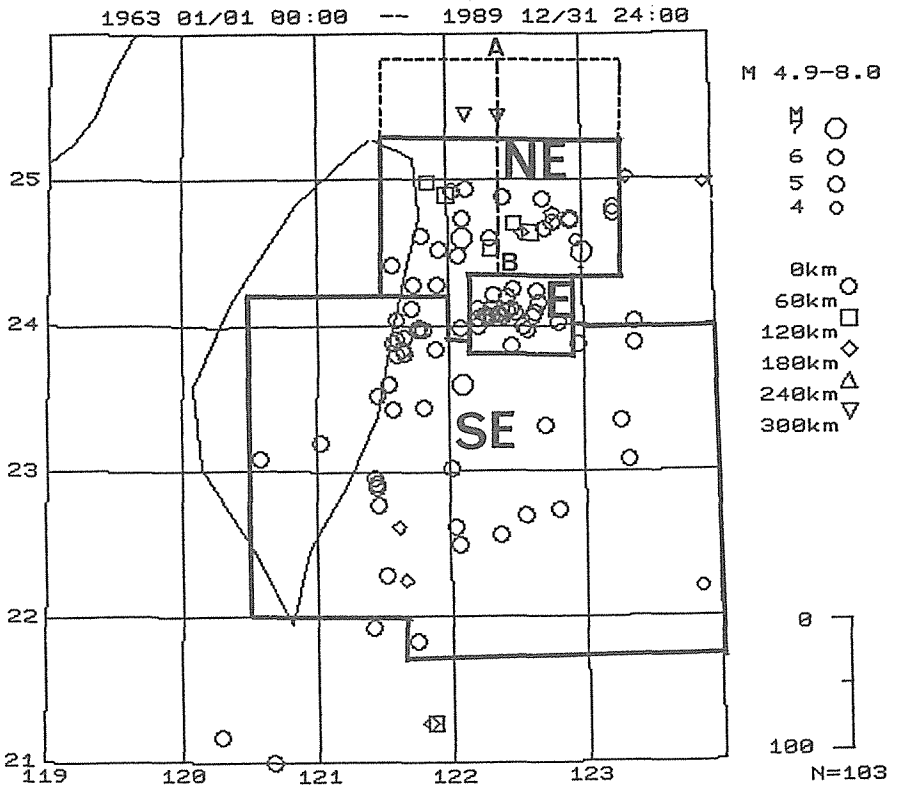

Fig. 4. Epicentral distribution of earthquakes with mechanism solutions and three seismic active regions related to the direction tendency of P-, T- and N-axes. They are southeastern (SE), eastern (E) and northeastern (NE) regions, respectively.

(SE), the eastern region (E) and the northeastern region (NE) of Taiwan. The southeastern region includes the main part of the Longitudinal Valley fault and the southeastern sea region. The eastern region is a small one located in the eastern sea off Taiwan near the cross of 122.5°E and 24.1°N. The northeastern region includes Hualian, the northeastern region of Taiwan and the northeastern sea region off Hualian.

The Wulff's net projections on the lower hemispheres of the P- (circles), T- (squares) and N-axes (crosses) of mechanism solutions of earthquakes occurring in each region are shown in Fig. 5. In the southeastern region (Fig. 5(a)), most of P- and N-axes lie horizontally in the WNW-ESE and the NNE-SSW directions, respectively. T-axes are in the vertical direction. The characteristics of the stress field in the southeastern region show that a horizontal compressive stress in the WNW-ESE direction is dominant, which is identical with the relative movement direction between the Philippine Sea and the Eurasian plates. The stress field in the eastern region is dominated by a near N-S horizontal compression, where P-axes have somewhat rotated northward compared to those in the southeastern region of Taiwan (Fig. 5(b)). Four mechanism solutions have the same characteristics as in the southeastern region, which

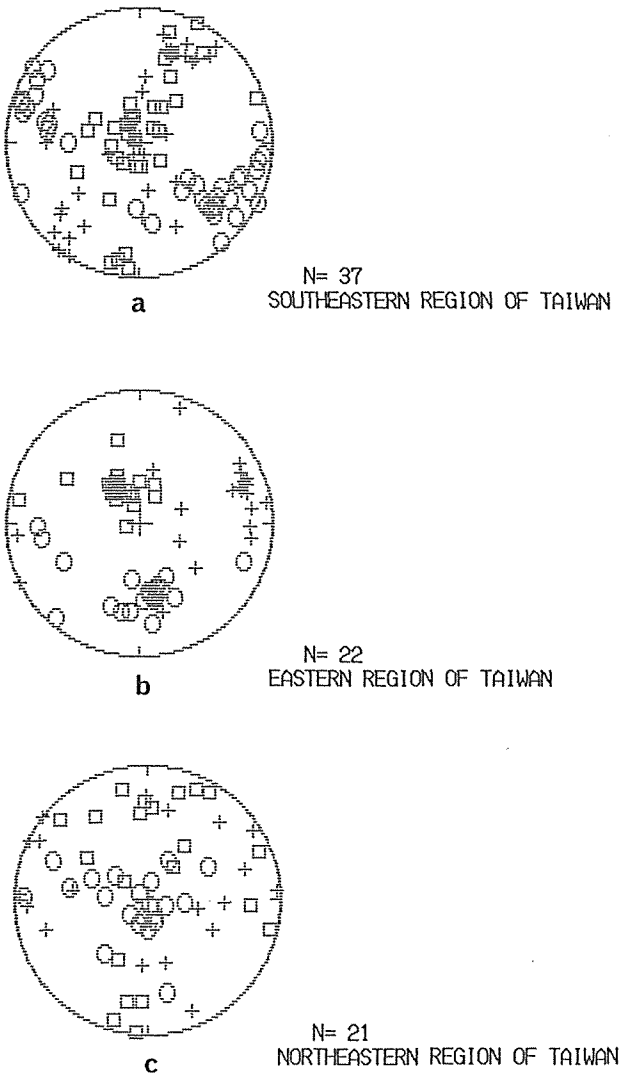

Fig. 5. Projections on the Wulff's nets of lower hemisphere of the P-axes (circles), T-axes (squares) and N-axes(crosses) in the southeastern (a), the eastern (b) and the northeastern (c) regions, respectively.

show P-axes in the WNW-ESE or near E-W directions and T-axes in the vertical direction. This can be considered that the compression force in the WNW-ESE direction due to the Philippine Sea plate influences upon the eastern region. Exceptionally one mechanism solution has P-axis in the NNE-SSW direction and T-axis in the vertical direction. Only shallow earthquakes shallower than 70 km depth occur in the SE and E regions as shown in Fig. 4. P-, T- and N-axes of shallow earthquakes in the northeastern region where a subduction zone exists as mentioned above, however, show different property from those for the other two regions. Most of the P-axes are concentrated on the vertical direction and T-axes lie horizontally in the N-S direction. The stress field in the shallow part of the northeastern region is dominated mainly by N-

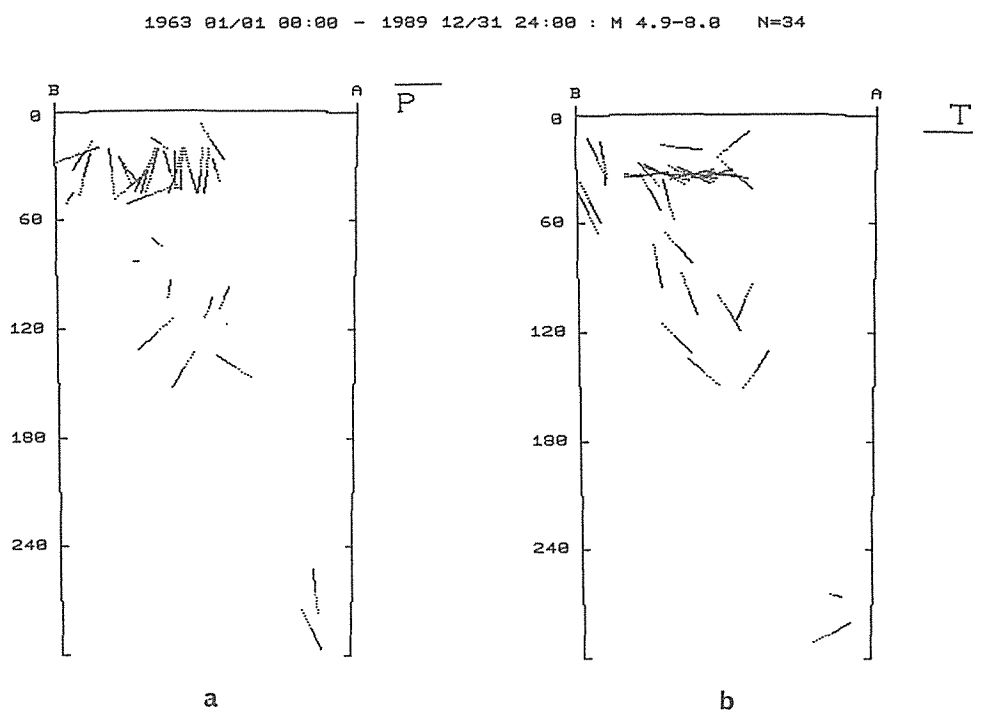

Fig. 6. Distribution of P- and T-axes on the vertical section along the AB line in Fig. 4.

S horizontal extension. This characteristic is similar to that in the shallow part of the subduction zones with down-dip extensional stress field. The N-S profile distributions of P- and T-axes along the slab are show in Fig. 6(a) and (b). Orientations of P-axes tend to be perpendicular to the slab inclination (a) and orientations of T-axes tend to be parallel to the slab inclination in the depth from the surface to the depth of 150 km, which implies that a down-dip extensional stress field exists in the upper part of the Benioff zone in the northeast sea of the Taiwan region. However, P- and T-axes of mechanism solutions of two deepest events occurring at 285 km show a different distributions with that in the shallower part. The P-axes are parallel to the slab (Fig. 6(a)) and the T-axes are perpendicular to the slab (Fig. 6(b)). This can be considered that the stress field changes from a down-dip extension in the shallow part to a down-dip compression in the deep part of the slab, as it reaches 280 km.

Two tectonic boundaries, the collision zone along the Longitudinal Valley fault and the subduction zone located beneath the northeastern sea region off Hualian, cross at Hualian region.

3. Finite Element Model

In order to study relationship among crustal deformation, seismicity, mechanism solution, stress field and the tectonic movement in and around Taiwan, tectonic deformation and stress field in the three-dimension are calculated using a finite element method.

A three-dimensional finite element method of elastic theory is employed to deal with a non-planar configuration of the collision between the Philippine Sea plate and Eurasian plate along the Longitudinal Valley fault, and the subduction of the Philippine Sea plate toward the Eurasian plate at the northeastern sea region off Hualian.

The three-dimensional finite element model has been realized based on hypocentral distribution of earthquakes, and tectonics in the Taiwan region. The horizontal projection of the finite mesh and taking X, Y and Z axes in a Cartesian coordinate system are shown in Fig. 7(a). The Y coordinate coincides with the trend of and partly along the Longitudinal Valley fault in the N20°E direction (Yu et al. 1990, Ho, 1986) as shown in Fig. 7(a). The southern boundary of the northeastern sea region is identical with the southern boundary of subduction zone based on the hypocentral distribution as shown in Fig. 3(a) and (b). The vertical projection of the finite mesh along AA′ in Fig. 7(a) is shown in Fig. 7(b). Based on depths of intermediate-depth earthquakes after 1936, the deepest finite mesh of the vertical profile in the northeastern part of Taiwan is taken as 285 km. According to the hypocentral distribution along the slab as shown in Fig. 3(b), the vertical projection of the finite element mesh along BB′ line in the subduction zone in Fig. 7(a) is shown in Fig. 7 (c). In this model, isoparametric elements with eight nodes is adopted (Yoshioka and Hashimoto, 1989, Yoshioka et al., 1989). The total numbers of the finite elements and

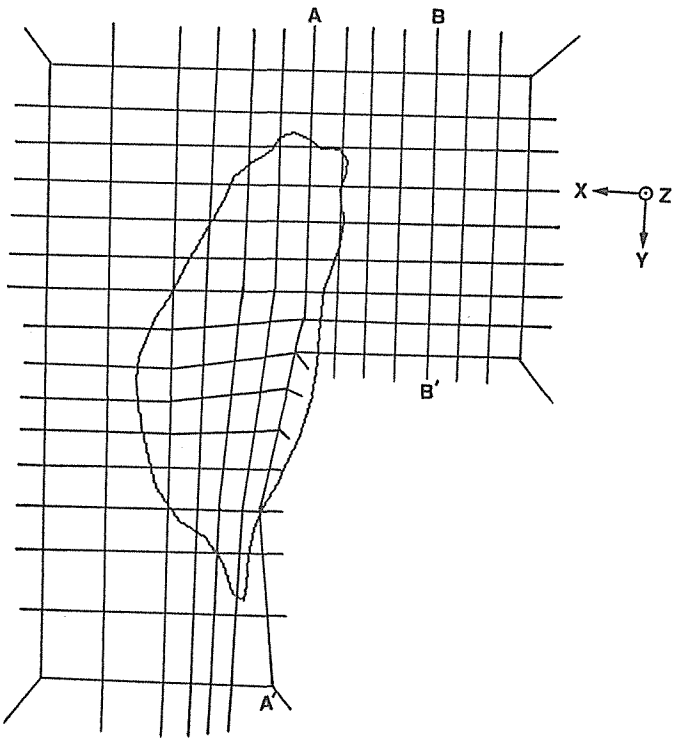

a

Fig. 7

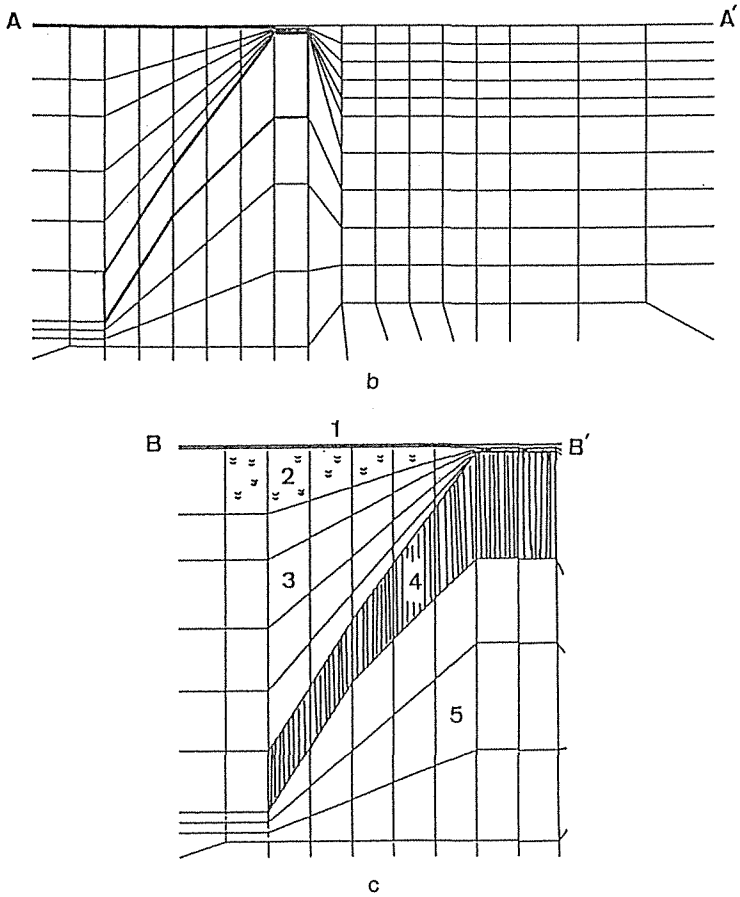

Fig. 7. (a) Horizontal projection of finite element mesh. (b) Vertical projection of finite element mesh along AA′ line shown in (a). The thick line shows the subduction zone in the northeastern sea region, which is made based on the hypocentral distribution along vertical projection. (c) Numerals from 1 to 5 correspond five materials to the Table 2.

Table 2. Material parameters

		Rigidity (dyne/cm^2)	Poisson's ratio	Density difference
1	ocean	0.5×10^{11}	0.40	−0.0900
2	crust	3.2×10^{11}	0.25	−0.0900
3	mantle wedge	4.7×10^{11}	0.30	−0.0245
4	slab	7.2×10^{11}	0.25	0.0667
5	asthenosphere	6.7×10^{11}	0.25	0.0000

nodes used in this study are 1460 and 1925, respectively.

In the model, ocean, crust, mantle wedge, slab and asthenosphere layers are shown by numbers from 1 to 5 in Fig. 7 (c), respectively. The material constants are given in Table 2. Material property is considered to belong to the elastic medium in this study.

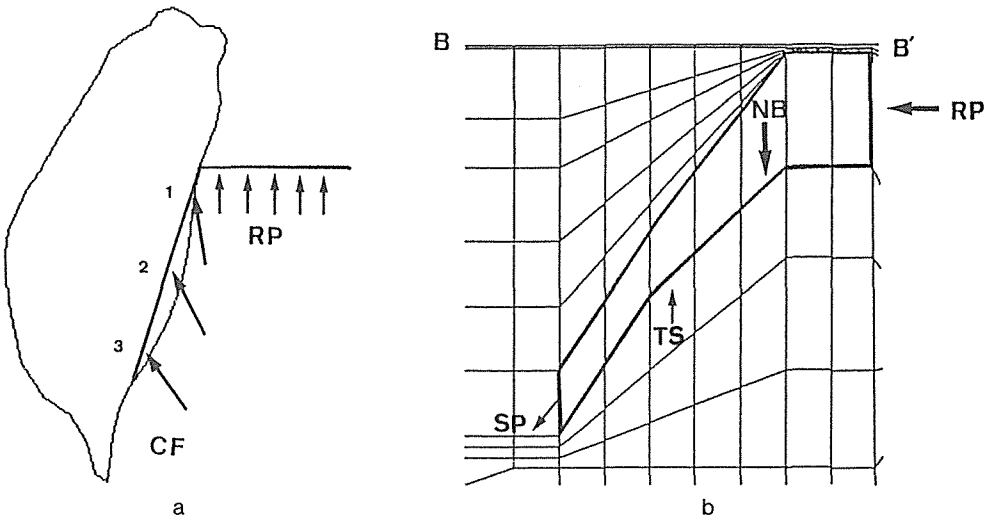

Fig. 8. Main five tectonic forces adopted in this calculation. They are : (a) a compression force in the azimuth 310° on the Longitudinal Valley fault (CF) and a northward ridge push force on the southern boundary of subduction zone (RP) generated by the movement of Philippine Sea plate toward Eurasian plate. (b) A negative buoyancy acting on the subduction zone (NB), a northward ridge push force (RP), a slab pull force exerted at the deeper part of the subduction zone (SP) and a thermal stress (TS).

Table 3. Stress Boundary Conditions (unit : bar)

		x	y	z
	1	239	−524	0
CF	2	248.5	−499.3	237.8
	3	177	−294	152.6
RP		0	−200	0
TS		0	0	150

Stress boundary condition has been employed in the calculation of the model established in the present study as shown in Fig. 8 and Table 3, which is derived from the observed crustal deformation data in Taiwan by Yu et al. (1990).

Several possible loads are proposed as follows and shown in Fig. 8(a) and (b).

(1) A northwestward compressive force generated by relative movement of the Philippine Sea plate to the Eurasian plate acting on the Longitudinal Valley fault in the shallower five layers from the surface to the depth of 75 km (CF in Fig. 8(a)). The direction and strength of the compressive force probably change along the fault.

(2) A negative buoyancy acting on the subduction slab beneath the northeastern sea region off Hualian due to the density contrast (NB in Fig. 8(b)), this is a body force.

(3) A northward ridge push acting on the plate layer in southern boundary of subduction zone generated by the evolution of the Philippine Sea plate (RP in Fig. 8(b)).

(4) A slab pull force exerted at the deeper part of the subduction zone due to the density contrast or the resultant of the pull force and the slab resistance (SP in Fig. 8(b)).

(5) Upheaval thermal stresses in the subduction slab which may be caused by the contact with a hot asthenosphere (TS in Fig. 8(b)).

In calculation of three-dimensional finite element model, each of these five tectonic forces is conducted respectively at first. A linear combination of the unitary calculated results for the five forces is then operated. The latter result is compared with the observed results until it coincides with the observed one.

4. Calculated Results of Displacement and Stress Field

Based on the three-dimensional finite element model and boundary tectonic conditions as mentioned above, the calculated results of the displacement and tectonic stress field are described as follows, respectively.

4.1. Displacements

The distributions of the calculated horizontal and vertical displacement in Taiwan are shown in Fig. 9 and Fig. 10, respectively. Figures (a), (b) and (c) indicate the results at depths of 10 km, 70 km and 150 km, respectively.

In the shallow part from the surface to the depth of 70 km in Taiwan, the horizontal

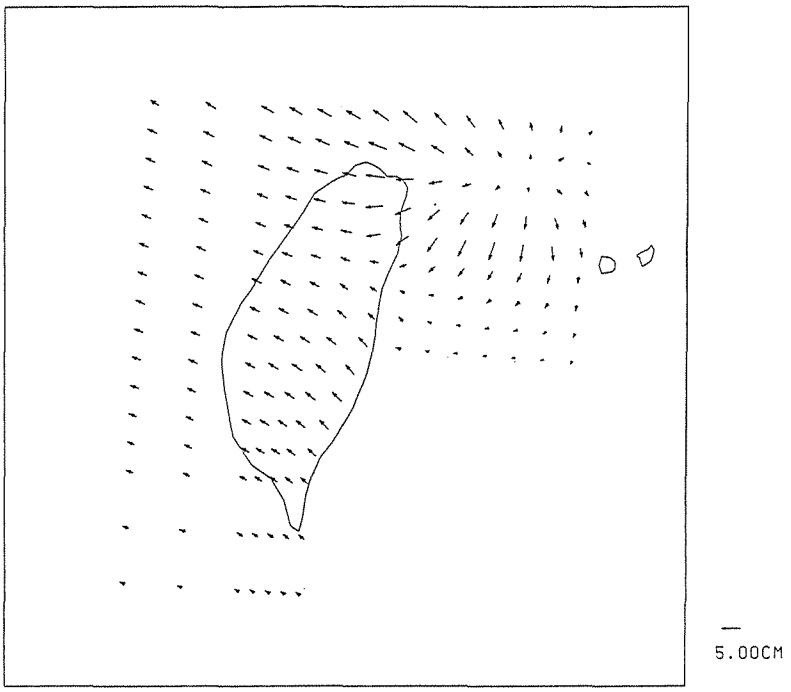

a

Fig. 9

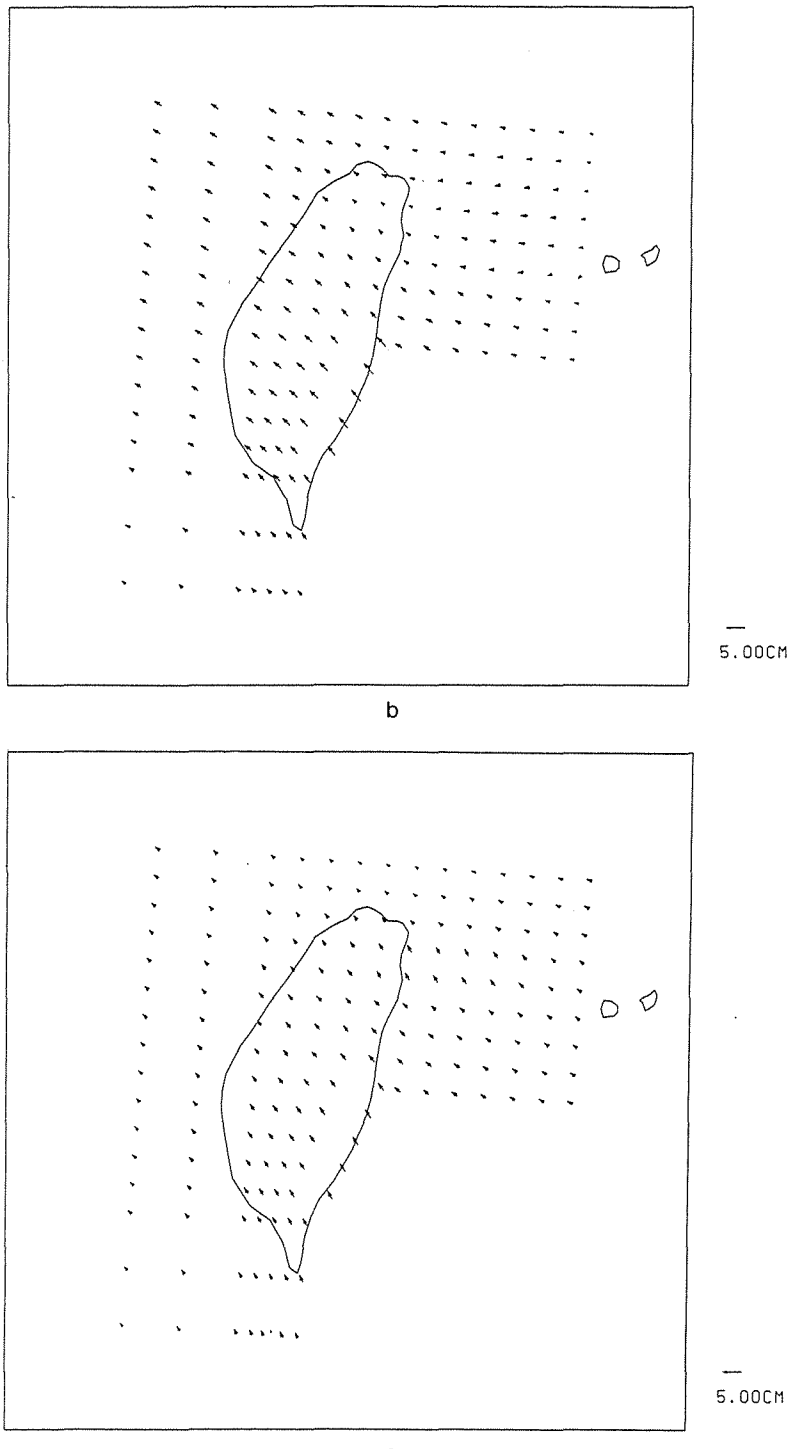

Fig. 9. Calculated results of horizontal displacements in the depth of 10 km (a), 70 km (b) and 150 km (c).

displacements have a regularity as shown in Fig. 9(a) and (b). The displacement directions rotate regularly from the NW-SE to the WNW-ESE direction from the southern and middle segments of the Longitudinal Valley fault to the central and western regions to west of the fault. The rates of horizontal displacement decrease from the Longitudinal Valley fault to the central and western regions, which change from about 4 cm/yr to 1 cm/yr. In this wide region the displacement field is controlled by northwestward compressive force generated by movement of the Philippine Sea plate acting along the Longitudinal Valley fault. Although the compressive force acts only on the crustal part in this calculation, the direction of horizontal displacement does not change down to the depth of 150 km and values of displacements decrease with depth.

In the shallow part of the northeastern sea region and northeastern region of Taiwan, the direction distribution of horizontal displacements at the depth of 10 km shows a gushing pattern from the blow part (Fig. 9(a)), the same pattern of the distribution appears at the depth of 30 km which is the middle part of the slab. This kind of distribution may be attributed to the negative buoyancy acting on the slab due to the density contrast of mediums and the thermal stress. When depth is greater than 30 km, the gushing pattern of horizontal displacement distribution can not been seen in the northeastern sea region off Hualian.

Figs.10(a), (b) and (c) show the vertical displacement distributions at the depth of 10 km, 70 km and 150 km, respectively. According to the direction of the vertical displacements, it is better to divided into two regions to analyze regionalcharacteristics.

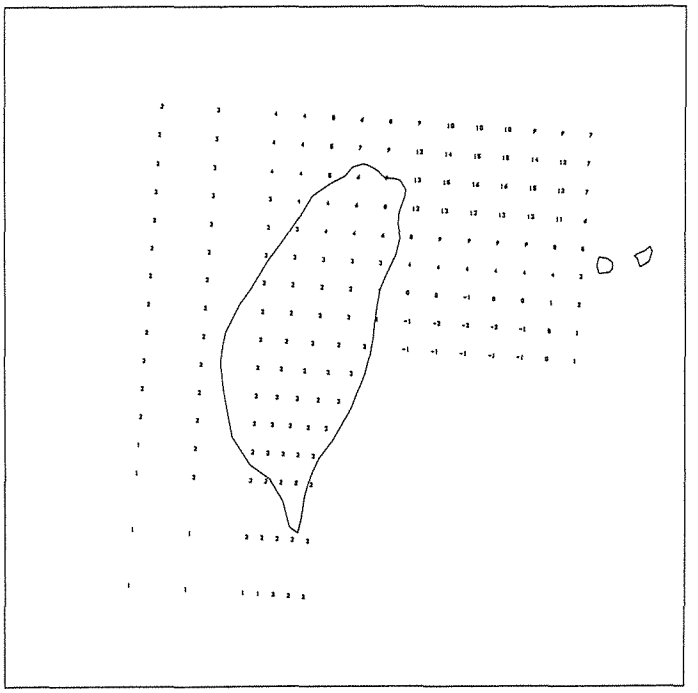

a

Fig. 10

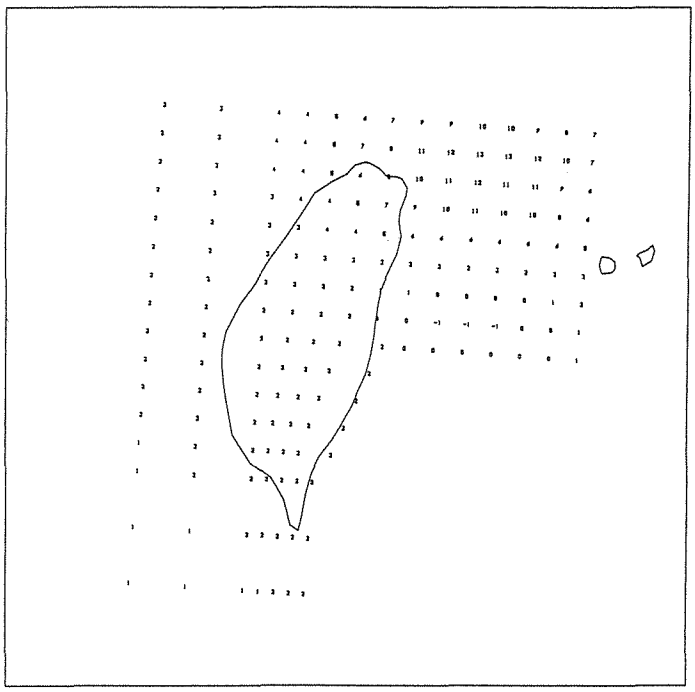

b

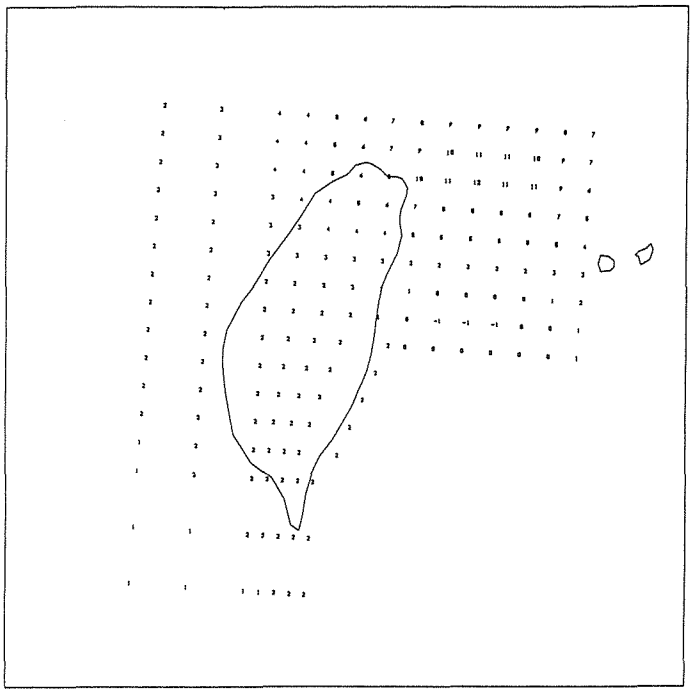

c

Fig. 10. Calculated results of vertical displacements in the depth of 10 km (a), 70 km (b) and 150 km (c).

One is a region from the Longitudinal Valley fault to the central and western regions located to west of the Longitudinal Valley fault. The other region includes the northern region and the northeastern sea region off Hualian.

Upheaval vertical displacements are simulated in the former region. The largest vertical displacement with value of 3 cm appears along the Longitudinal Valley fault. The values of the vertical displacement decrease with distance away from the fault from east to west (Fig. 10(a)). The decrease of the vertical displacement is obviously corresponding to the Philippine Sea plate acting along the Longitudinal Valley fault. The upheaval vertical displacements decrease in deep parts. At the depth of 150 km, the values of the vertical displacement along the Longitudinal Valley fault are about two third of those at the depth of 10 km (Fig. 10(c)).

The vertical displacement is interesting in the northern region of Taiwan and the northeastern sea region off Hualian. A subsidence vertical displacements appears in the southern region of the subduction zone (Fig. 10(a), (b) and (c)), whose values are from 0 to −2 cm in the depth of 10 km. A upheaval vertical displacements, however, is simulated in the northern region of Taiwan and the northern region of the subduction zone beneath the northeastern sea region. The value of upheaval vertical displacement is 16 cm in the central part of the subducting slab at the depth of 10 km deep layer, which is the largest one in the Taiwan region.

The large difference of the vertical displacement is simulated in the shallow part (shallower than 50 km) between the northern and the southern regions. At 150 km deep, the difference of vertical displacement decreases between the part beneath the southern region of subducting slab and the northern region and the northeastern sea region off Hualian (see Fig. 10(c)).

4.2. Stress Field Patterns

Calculated stress field patterns are shown in Fig. 11. Figures (a), (b) and (c) show the results at the depths of 10 km, 70 km and 150 km, respectively. The stress field pattern is indicated by earthquake focal mechanism on the Wulff's net projections (lower hemisphere).

At the depth of 10 km, large compressive stress appear along the Longitudinal Valley fault in the Taiwan region, especially in the region between Yuli and Hualian. The largest value of the compressive stress at the depth of 10 km is about 200 bars in the region between Yuli and Hualian (Fig. 11(a)). The stress field along the Longitudinal Valley fault shows a thrust faulting pattern, for which P-axes are in the WNW-ESE or almost E-W directions. The pattern is identical to observed results of Xu et al. (1989) and the solutions previously discussed in this paper. The stress in the northeastern sea region are less than that along the Longitudinal Valley fault at the depth of 10 km. The stress field pattern there reveals a normal faulting type.

Fig. 11(b) and (c) show the distributions of stress field at the depths of 70 km and 150 km, respectively. The compressive stress decrease when depth increase along the Longitudinal Valley fault, though the stress field patterns do not change. The tensile stress increase in the Hualian and the northeastern sea region when depth increases. At the depth of 70 km, the value of tensile stress in the subduction zone are equal to the

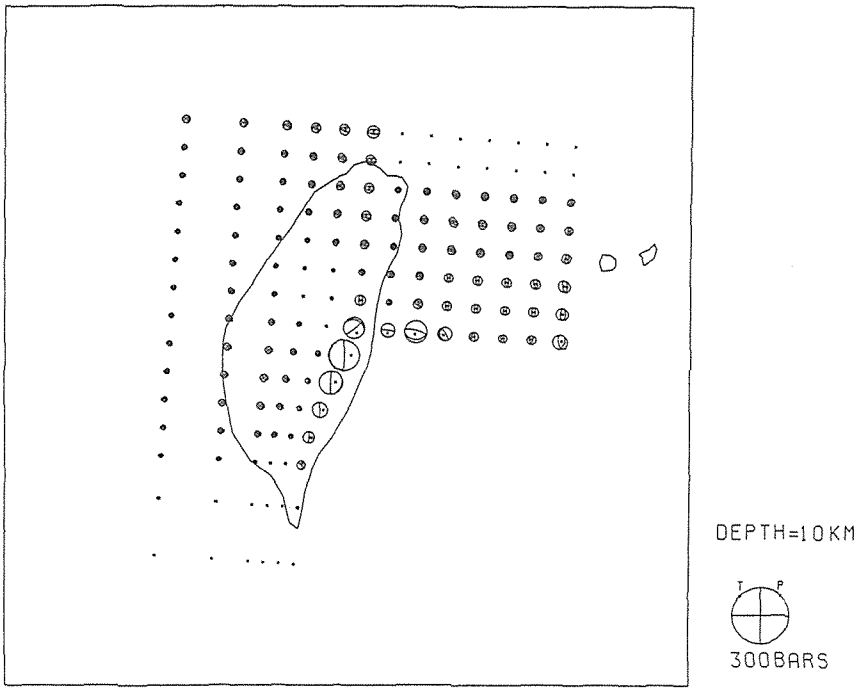

a

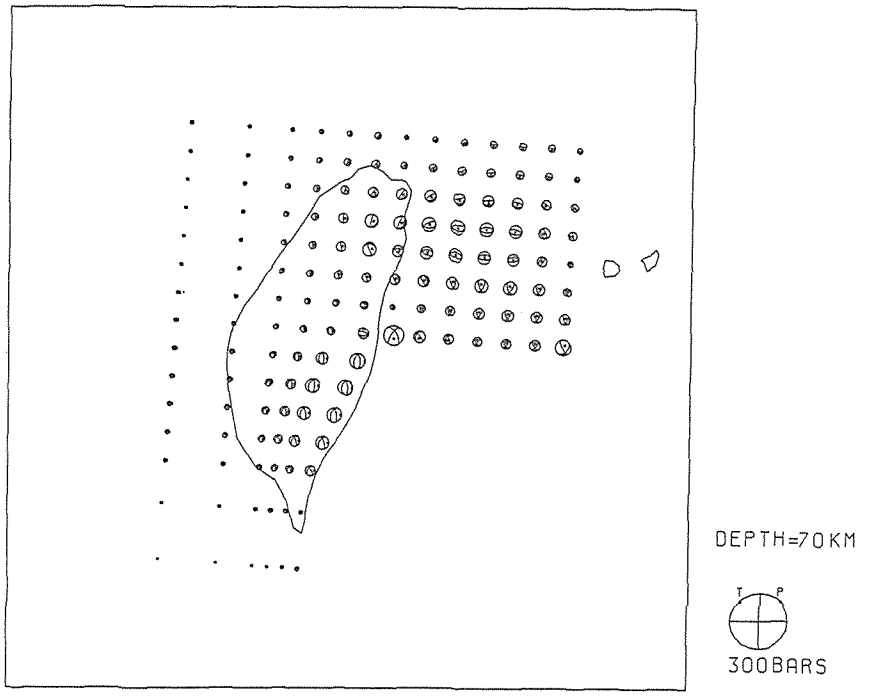

b

Fig. 11

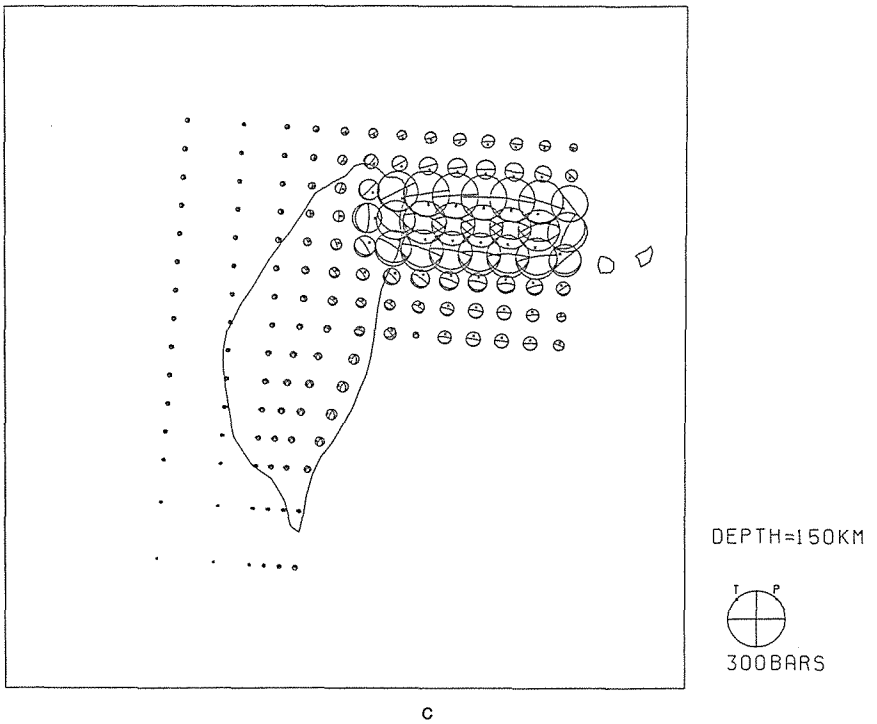

Fig. 11. Distributions of calculated horizontal stress field in the depth of 10 km (a), 70 km (b) and 150 km (c).

compressive stress along the Longitudinal Valley fault. At the depth of 150 km, the values of tensile stress in the subduction zone are larger than the compressive stress along the Longitudinal Valley fault.

In the Hualian and the northeastern sea region off Hualian, the calculated result shows that a down-dip extension stress field is dominant within the whole slab. In the shallow part from 10 km to 70 km, calculated P-axes are perpendicular to and T-axes are parallel to the surface (Fig. 11(a) and(b)). At the depth of 150 km, the stress within the slab shows that T-axes are in the vertical direction and P-axes lie in the horizontal N-S direction (Fig. 11(c)). Because the bending slab turns to the nearly vertical direction in 150 km deep, T-axes are also within the slab in the deeper part of slab. The values of stress within the slab are larger than that of surrounding region. The calculated results probably explain why earthquakes, especially the intermediate-depth earthquakes, tend to occur within the slab.

5. Discussion

Taiwan region is a young orogenic belt in geology (Ho, 1986). The orogenic movement continues up to the present under the strong compressive force caused by the Philippine Sea plate. The coastal and central ranges are upheaval in rates of about 5 cm/yr and 2 cm/yr, respectively (Wang, 1987).

The calculation in the present study coincides with observations in seismology and geotectonics, therefore the proposed forces in the model may represent the seismogenic force in the Taiwan region and its surrounding.

5.1. Compression Along the Longitudinal Valley Fault and Tension in the Hualian and the Northeastern Sea Region

The model with tectonic force system shows that the crustal stress field along the Longitudinal Valley fault and the central and western region to west of the fault are controlled by compressive stress from the collision of the plates. In this region, calculated stress field reveals that a compressive stress field produces thrust faulting type events and P-axes lie in the WNW-ESE direction, which coincides with observed focal mechanisms. The compressive force CF in the model (Fig. 8) is supposed to come from the relative movements between the Philippine Sea and Eurasian plates in the Taiwan region (Seno and Kurita, 1979, Lin et al., 1985, and Huchon et al., 1986). Therefore, both earthquake generating natures, and directions of P-axes and T-axes of stress field can be considered to be controlled by the movements of the Philippine Sea plate to the Eurasian plate.

For a case of the Hualian and the northeastern sea region, the model with five tectonic conditions can explain the tensile stress field there in the shallow part well. Among the five tectonic conditions, the negative buoyancy NB (Fig. 8) due to low crustal density and the upheaval thermal stresses TS (Fig. 8) on the slab caused by the contact with a hot asthenosphere play an important role. A buoyant force gives a isotropic horizontal tensile stress and upheaval thermal stress increases the tensile stress in the shallow part of the slab in the northeastern sea region off Hualian. The negative buoyancy NB and the upheaval thermal stresses TS also can generate a upheaval force acting on the bottom of bent part of slab obviously.

The calculated results show that the down-dip extension exists along the whole bending subduction zone to the depth of 150 km. This is identical to observations as mentioned above in the Hualian and the northeastern sea region. In the shallow part over the subduction zone, the tensile stress being parallel to the slab i.e. the surface in the direction of N-S play an important role for the generating of normal faulting type earthquakes, explaining why the normal faulting events in depth range from the surface to 70 km occurred concentratelly and the T-axes lie in the N-S direction. In the intermediate-depth part of slab, the horizontal component of compressive stress in the N-S direction becomes large enough to control the earthquake occurrences. Under this stress, the mechanism solutions of intermediate-depth earthquakes show the reverse faulting type ones (around 100 km). The calculated results coincide with the observations.

At the depth of 280 km, the P-axes of focal mechanisms turn to parallel to the slab (Fig. 6(a)) and the T-axes turn to perpendicular to the slab (Fig. 6(b)). A down-dip compression appears in the deep part of the slab beneath the northeastern sea region of Taiwan. This change of stress within the slab may be attributed to the slab penetrating and encountering with resistance from stronger material in the deeper part. The down-deep compression controls the stress field in the deepest part of the slab.

In summary, the down-dip extension exists the slab from the surface to about 200 km deep, which results from the gravitational force due to density difference between the slab and its surrounding, the thermal stresses on the slab caused by the contact with a hot asthenosphere and so on. At the depth of about 300 km, the down-dip compression, which may be caused by compression resulted from the presence of the strong material in the deep part.

It is shown in Fig. 11 that the large compressive stress exist along the Longitudinal Valley fault and decrease when depth increases. In northeastern sea region, the large stress along slab exist in the deep. It can explain that the former is caused by the collision and the latter is caused by the subducting movement between the Philippine Sea plate and the Eurasian plate.

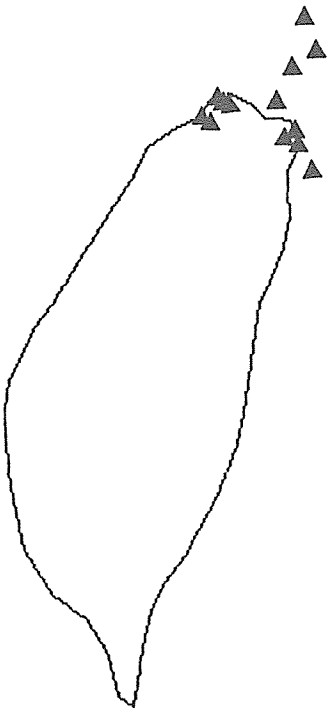

Fig. 12. Volcanoes and volcanic islands in Taiwan region.

The inversion results of three-dimensional P and S waves velocity structures show that a high velocity region exists in the northeastern region and the northeastern sea region in Taiwan (Roecker er al., 1987). There are some extinct volcanoes in the northern region of Taiwan and small islands to north of the Hualian region (Wang, 1987) (Fig. 12). The Hualian region is a famous hot spring region and a high heat flow anomalies region in Taiwan too. It shows that there are some features of subduction zones in the northeastern sea region off Hualian in Taiwan. These evidences coincide with the seismic observations in the present study. The subduction movement between the two plate influences on the seismogenic stress field in the northeastern sea region off Hualian.

5.2. Distribution of Horizontal and Vertical Displacements

The calculated horizontal and vertical displacements along the Longitudinal Valley fault and the central and western region to west of the fault coincide with the results of observation on whole (Yu, 1990). The strong compression force from the Philippine Sea plate causes crust to move horizontally in the WNW-ESE or nearly E-W direction with an upheaval displacement component along the Longitudinal Valley fault. The largest rates of horizontal and vertical displacements are about 3.5 cm/yr and 2–3 cm/yr along the fault, respectively. In the western region, the calculated crustal displacement perhaps are somewhat larger than observations. This difference is probably attributed to some difference between the elastic model adopted in this study and an incomplete elastic earth medium.

Concerning the Hualian and the northeastern sea region, because most area is in the sea, it is difficult to survey the crustal displacement by the triangulation and leveling survey. The calculated displacement shows a interesting distribution in and around the subduction zone. The upheaval displacements are located in the northern region of the subduction zone, in which the largest one appears above the central area of the slab. The distribution of displacement may related to the subduction movement in this region.

6. Conclusions

Displacement and stress field simulated from the three-dimensional finite element model in the Taiwan region established in this paper are concluded as follows.

(1) There is a compressive stress field in the WNW-ESE direction along the Longitudinal Valley fault and the central and western region west of the Longitudinal Valley fault. It is attributed to the compressive force in the WNW-ESE direction generated by the collision movement between the Philippine Sea plate and the Eurasian plate. The reverse faulting is dominant in shallow earthquakes along the fault.

(2) In the northeastern sea region off Hualian, a northward-dipping Wadati-Benioff zone exists along 24°N, which has the thickness of about 60 km and begins to deepen from 24°N at dip angle of 45° to 50°. The leading edge reaches a depth of about 300 km at about 25.5°N. The presence of such seismic zone implies that subduction of the Philippine Sea plate under the Eurasian plate extends from south to north in the northeastern sea region of Taiwan. A down-dip extensional stress exists within the slab from the surface to about the depth of 200 km, which results from the gravitational force due to density difference between the slab and its surrounding, the thermal stresses on the slab caused by the contact with a hot asthenosphere. In the crust shallower than 70 km, a tensile stress exists in the N-S direction, which is attributed to the down-dip extension. The normal faulting shallow earthquake dominates seismic activity there. At the depth of about 300 km, the stress within the slab changes from the down-dip extension to the down-dip compression. It may come from the presence of the strong material in the deep part.

(3) Displacement fields are different between the two regions mentioned in conclusion (1) and (2). The former is of the horizontal upheaval in the WNW-ESE

direction. It has been controlled by the compressive movement of the Philippine Sea plate. Complex displacement appears in the latter region. The subsidence exists in the southern region of the slab and the upheaval exists in the northern region of the slab.

(4) The Hualian region is located at a cross of boundaries, i.e. the collision zone along the Longitudinal Valley fault and the subduction zone under the northeastern sea region off Hualian. Therefore, it is a high seismically zone as well as a complex stress pattern zone.

The author is very grateful to professor Kazuo Oike for helpful suggestions and comments. I would like to thank Dr. Shoichi Yoshioka for providing his program and giving valuable helps. I wishes to express my thanks to professor Yeeng-Tein Yeh for valuable helps. I also would like to thand Dr. Zhixin Zhao and Dr. Keiko Kuge for their fruitful discussions.

Calculations in this study were carried out using the computer systems at the Data Processing Center, Kyoto University.

References

Angelier, J., E. Barrier and H.T. Chu, Plate collision and paleostress trajectories in a fold-thrust belt : the foothills of Taiwan, *Tectonophysics,* **125**, 161–178, 1986.

Dziewonski, A.M. and J.H. Woodhouse, An experiment in systematic study for global seismicity : centroid-moment tensor solutions for 201 moderate and large earthquakes of 1981, *J. Geophys. Res.*, **88**, 3247–3271, 1983(a).

Dziewonski, A.M., A. Friedmen, D. Giardini and J.H. Woodhouse, Global seismicity of 1982 : centroid-moment tensor solutions for 308 earthquakes, *Phys. Earth Planet. Inter.*, **33**, 76–90, 1983(b).

Gu, G.X., T.H. Ling and Z.L. Shi, Seismological Catalogue of China, (B.C. 1831–A.D. 1969), Science Press, Beijing (in Chinese), 1983(a).

Gu, G.X., T.H. Ling and Z.L. Shi, Seismological Catalogue of China, (1970–1979), Seismological Press, Beijing (in Chinese), 1983(b).

Group for Seismological Almanac of China, Seismological Almanac of China of 1982, Seismological Press, Beijing (in Chinese), 1985.

Ishikawa, Y, The tectonics in East Asia inferred from seismicity and focal mechanism of earthquakes (in preparation), 1993.

Ho, C.S., Synthesis of the geologic evolution of Taiwan, *Tectonophysics,* **125**, 1–16, 1986.

Huchon, P., E. Barrier and J.C. De Bremaecker, Collision and stress trajectories in Taiwan : a finite element model, *Tectonophysics,* **125**, 179–191, 1986.

Hsu, V., Seismicity and tectonics of a continent-island arc collision zone at the island of Taiwan, *J. Geophys. Res.*, **95**, 4725–4734, 1990.

Lin, C.H., Y.H. Yen and Y.B. Tsai, Determination of regional principal stress directions in Taiwan from fault plane solutions, *Bull. Inst. Earth. Sci., Academia Sinica,* **5**, 67–85, 1985.

Melosh, H.J. and A. Raefsky, A simple and efficient method for introducing faults into finite element computations, *Bull. Seismolo. Soc. Am.*, **71**, 1391–1400, 1981.

Pezzopane, Silvio K. and Steven G. Wesnousky, Large earthquakes and crustal deformation near Taiwan, *J. Geophys. Res.*, **94**, 7250–7264, 1989.

Roecker, S.W., Y.H. Yeh and Y.B. Tsai, Three-dimensional P and S wave velocity structures beneath Taiwan : Deep structure beneath an arc-continent collision, *J. Geophys. Res.*, **92**, 10, 547–10, 570, 1987.

Sheu, H.C., Crustal movements of South Okinawa Trough and Nan area, Taiwan, Journal of Surveying Engineering, Vol. 29, No. 3, 1–6, 1987.

Seno, T., The instantaneous rotation vector of the Philippine Sea plate relative to the Eurasian plate, *Tectonophysics,* **42**, 209–226, 1977.

Seno, T. and K. Kurita, Focal mechanismas and tectonics in the Taiwan-Philippine region, *J. Phys. Earth,* **26**, pp. 249–265, 1979.

Tsai, Y., Seismotectonics of Taiwan, *Tectonophysics,* **125**, 17–37, 1986.

Wang, S.Y. and Z.H. Xu, Seismo-tectonic stress field in East China, *Acta Seismologica Sinica,* Vol. 7, No. 1, 17–32 (in Chinese), 1985.

Wang, J.H., An interpretation to the first-motion solution of microearthquakes in the southern I-Lan, Taiwan, *Bull. Geophy., Central Univ., ROC,* No. 26, 85–106, 1984.

Wang, X., The special geological landscape in Taiwan (from author, private communication), 1987.

Xu, J.R, Z.X. Zhao, K. Oike and Y. Ishikawa, Properties of the stress field in and around West China derived from earthquake mechanism solutions, *Bull. Disas. Prev. Res. Inst., Kyoto Univ.,* **38**, Part 2, 49–78, 1988.

Xu, J.R., Z.X. Zhao, K. Oike, and Y. Ishikawa, Regional characteristics of focal mechanisms of shallow earthquakes in and around China, Proceeding of the Japan-China (Taipei) Joint Seminar on natural hazard mitigation, 16–20, 1989.

Yan, J.Q., Z.L. Shi, S.Y. Wang and W.L. Huan, Some features of the recent tectonic stress field of China and environs, *Acta Seismologica Sinica,* Vol. 1, No. 1, 25–38 (in Chinese), 1979.

Yoshioka, S. and M. Hashimoto, The stress field induced the occurrence of the 1946 Nankaido earthquake, and their relation to impending earthquakes, *Phys. Earth Planet,* **59**, 349–370, 1989.

Yoshioka, S., M. Hashimoto, and K. Hirahara, Displacement field due to the 1946 Nankaido earthquake in a laterally inhomogeneous structure with the subducting Philippine Sea plate — a three-dimensional finite element approach, *Tectonophysics,* **159**, 121–136, 1989.

Yu, S.B., D.D. Jackson, G.K. Yu and C.C. Liu, Dislocation model for crustal Deformation in the Longitudinal Valley area, Eastern Taiwan, *Tectonophysics,* **183**, 97–109, 1990.

Zhao, Z.X., K. Oike, K. Matsumura and Y. Ishikawa, Stress field in the continental part of China derived from temporal variations of seismic activity, *Tectonophysics,* **178**, 357–372, 1990.

Zhuo, S.R. and G.T. Chen, On the focal mechanisms of earthquakes and regional stress field of the Fujian-Taiwan region, *Acta Seismologica Sinica,* Vol. 5, No. 4, 397–411 (in Chinese), 1983.